

PITTING CORROSION SUSCEPTIBILITY OF SUPER AUSTENITIC STAINLESS STEELS IN SEA WATER

C.A. Loto

Department of Mechanical Engineering
University of Lagos, Akoka
Lagos, NIGERIA

ABSTRACT

Pitting corrosion susceptibility of some super austenitic stainless steel tubes exposed to flowing sea water in a specially designed test rig was investigated by field tests and laboratory analyses. The middle part of the steel tubes was put under elevated temperature in the steam chamber part of the rig. The tubes brought to the laboratory were examined with the Wild M3C Model optical macro/microscope after splitting and cleaning. The scanning electron microscopy, (S.E.M.) was used to examine and analyse the observed microscopic pits and microbiological organisms. EDAX (Energy Dispersive X-ray spectrometer), and the X-ray Diffraction spectroscopy (XRD) analyses were performed on the biofilm at the outlet-portion of some of the tubes. This paper reports the observed pitting corrosion behaviour of the tubes' alloys. Pitting corrosion susceptibility was found to be generally very minimal except for the 316L alloy which was used for comparison purpose.

Key Words: Pitting, corrosion, super austenitic stainless steels, tubes, sea-water.

INTRODUCTION

In a very recent paper⁽¹⁾, the under-deposit corrosion under the calcareous deposit on the steel surface in sea water was reported for some different types of super austenitic stainless steels. The under-deposit corrosion occurred, solely in the steam chamber portion of the tubes in the test rig and the observed corrosion was macroscopically visible.

The present report is a continuation of the one briefly described above. This work investigates the pitting corrosion susceptibility of the tested alloy tubes at the steam outlet portion of the tubes. The general observation was that slimy biofilm was present at this section of the tubes which also experienced lower temperature when compared with the

steam chamber section where adherent calcareous deposit occurred to cause severe under-deposit corrosion.

Due to the presence of slimy biofilm at this section of each of tested tubes, the presence and influence of the bacterial activity was also briefly examined by the use of the scanning electron microscopy; and the biofilm composition was analysed with Energy Dispersive X-ray (EDAX) and the X-ray diffraction spectroscopy (XRD).

Experimental Procedures

The experimental methods in this report follow the previously reported work⁽¹⁾ on this research subject. Nine tubes, each 2.14 metres long and 19mm dia, made of different alloys of varying chemical composition - Table 1,⁽¹⁾ were used for the field test. The tubes were specially fitted in a specially designed test rig located at the HBOI - Harbor Branch Oceanographic Institution, Florida in such a way as to permit uniform flow of sea water which was being pumped through. Located in about the middle portion of the tubes' length, was a steam chamber about 0.305 metres long, at which a pre-determined steam temperature was maintained. Several test runs each lasting for 60 days averagely, were made. The pre-determined water flow rate varied from one test run to another. After each run, the tubes were brought to the laboratory after cutting to some specified lengths, for further examinations and analyses. Table 2 gives a summary of the field test operating parameters.

Samples of the as-received stainless steels which were used in the test, were examined with the low power micro/microscope - Wild M3C model and the scanning electron microscope (S.E.M.) to determine the pre-test surface condition(s).

The cut tubes from the field test, brought to the laboratory were each split into two with the weldment being at one point. The split tubes were then cleaned with water detergent solution and hand brush. Photographs of the split tubes were taken in some instances before and after cleaning, before further examination with the Wild M3C Model optical macro/microscope. The macroscope was used to observe the whole length surface of each tube to locate the presence of any corrosion pit or local corrosion attack site. Some of the microscopic corrosion pits' micrographs were taken with the scanning electron microscopy (S.E.M.).

Examinations were also made of the rings cut from the in-let and the outlet sides of some of the tubes. The cut rings which were brought to the laboratory, and kept in glutaraldehyde in small plastic bottles were subjected to critical point drying in CO₂ atmosphere. They were then cut into test specimens of about 20mm and 25mm. The test specimens were examined in the S.E.M. in turns, after gold plating; and the observed surface containing bacteria or other microorganisms were photographed.

EDAX and XRD analyses of the biofilm, local corrosion attack sites composition and the bare metal were performed on some of the specimens.

Results

The as-received tubes surface, for example as in Figs. 1(a) and 2(a) were rough with etch-like appearance. The grain boundaries were microscopically visible in some cases. A comparison of some of the tubes surface before and after the test shows some distinct difference with respect to changes in surface feature(s), Fig. 1(b) and 2(b). In particular, sites of local corrosion attack could be located in the tested 316L alloy.

The biofilm in the steam chamber section of the tested tubes was either very light, non-existent or with strong adherent calcareous deposit as observed in one of the test runs. The latter phenomenon had been the major subject matter of the previous report⁽¹⁾. The results reported here are based more on the observations in the tubes' outlet portion and also the inlet portion. An example of a set

of the split and cleaned test tubes is presented in Figure 3. The super austenitic stainless steels were very corrosion resistant in general, with respect to pitting corrosion.

All the steel alloys corroded slightly with very little microscopic pits in the steam outlet portion. Quite a number of microscopic pits or sites of local corrosion attack were obtained along the weldment of the tubes made with AL6XN (NO8367) alloy in all the test runs as exemplified in Fig. 4. The 1925 HMO (NO8925) steel alloy was very resistant to pitting corrosion, though it suffered under-deposit corrosion in the steam chamber portion. The 254 SMO steel alloy was also very resistant to pitting corrosion. A ring form of local corrosion attack was, however, once obtained in its outlet portion, Fig. 6. Though, not a super austenitic stainless steel due to its relatively lower Mo content, the 316L (S31603) alloy was used along with the other steel alloys for comparison purpose. It failed visibly in all the test runs. In many cases, a cluster of pitting corrosion was observed; the pits were fairly deep penetrating and some times, perforation(s) occurred. An example of a microscopic pit observed in this steel is presented in Fig. 7. The corrosion pits observed in all the super austenitic stainless steels were not deep penetrating. They were shallow, flat, and some roundish.

Bacteria/microorganisms were obtained in all the test specimens, within the biological materials' matrix located on the tube's surface, Fig. 8-11. Though not absolutely the case, the denser biological materials were obtained at the portions that were known to contain more local corrosion attack sites. An example of the results obtained from the EDAX analysis performed on some of the specimens' surface is presented in Fig. 12. X-ray diffraction analysis of one of the tubes' outlet biofilm is presented in Fig. 13.

Discussion

In the previous report⁽¹⁾, attention was paid to what happened in the steam chamber with respect to severe underdeposit corrosion under the calcareous deposit in one of the test runs. In this report, attention has been paid more to what happened out-side the steam chamber than inside the steam chamber portion of the tubes; particularly the steam outlet and in-let portions where there was slimy biofilm

without any calcareous deposit, and where microscopic pits occurred; and tubercles present in the 316L steel alloy. The water flowing through the steam outlet was also at elevated temperature.

Surface examination of the cut tube specimens shows the effect of the sea water modification on some of the tested tubes, either by creating local corrosion attack sites, Fig. 2 or opening up the previously etched grain boundaries. When examined with the scanning electron microscope (S.E.M.), no particular form of inclusion was observed in any of the as-received test specimens. It could not therefore be said that surface preparation or characteristics contributed in any significant way to any pitting corrosion observed.

All the steel alloys were relatively very corrosion resistant in sea water except the 316L which has lower Mo content. Corrosion pits could not be identified distinctly in 904L and 254 SMO alloys. The AL6XN alloy had microscopic corrosion pits, all along the weldment. This could be due to welding defects during fabrication. Though no deep penetration of any of the pits could be observed, the long term effect is very difficult to determine. However, the pitting condition did not seem to pose any danger during a short term use.

The corrosion attack resistance of all the alloys tested except the 316L, was due to the very high alloying contents of the steels - and particularly, the Mo, Cr, Ni, N and to some extent, Si and Mn. These metallic elements are known (2-10) to provide stable passivity for the corrosion resistance of these super austenitic stainless steel alloys in corroding media. The high Mo content, in particular, has been recognised as having very high and stable passivating effect⁽²⁻⁶⁾.

In the scanning electron micrographs provided for the presence of bacteria, Fig. 8-11 no bacteria colony could really be conspicuously seen. Apart from the dense biological materials on the steels surface covering the bacteria, the method of preserving them from the field to the laboratory in glutaraldehyde, combined with the steps involved in critical point drying caused the bacterial destruction and loss substantially. However, some could still be observed. Their influence on the pitting corrosion observed

could not be fully assessed. There were more pitting corrosion and tubercles, for example, on 316L alloy tube, than in others; and more bacteria were found within the corrosion pits than outside the pits of alloy. Comparatively, more bacteria were observed on the 316L tube surface than in the other alloys. This observation probably suggests that bacteria had some influence on the rate and/or magnitude of corrosion.

The bacteria and other microbiological organisms were present mainly under the biofilms and the slimy biological materials where some bacterial activity would certainly be in process. This in combination with the high chloride ions from the sea water; and the carbonate and sulphate ions, would cause the depassivation of the tubes' metal passive film, creating anodic and cathodic sites for anodic and cathodic corrosion reactions to occur. The pitting corrosion observed would therefore be of synergism mainly between the chloride ions and bacterial activities.

The EDAX analysis, Fig. 12, confirms the presence of different chemical elements and these include Si, P, Ca, Na in addition to Cr, Mo, Ni etc. Sulphur could not be detected distinctly as it shares the same signal with Mo and it is also being marred by the gold (Au) used in locating the specimen surface. The effects of these elements are not clearly known. While the chloride ions (Cl⁻) from the sea water would make a significant contribution towards the depassivation of the alloys' protective film, others such as Cr, Ni, Mo, and Si were presumably giving protective effects of stabilising the alloys passive film, and at the same time, preventing the biofilm's growth that could lead to increased corrosion.

The X-ray diffraction analysis, Fig. 13 confirms the presence of CaCO₃, NaCl and FeOOH in the outlet biofilm. Since no significant corrosion was observed in the alloys except the 316L, the effects of these chemical compounds on the corrosion resistance or pitting corrosion susceptibility of these alloys could not be ascertained.

Conclusion

The pitting corrosion susceptibility of the super austenitic stainless steels in sea water was very minimal despite the presence of slimy biofilms and dense biological materials.

Alloys 254 SMO (S31254), 1925 HMO (NO8925) and 904L (NO8904) showed very good pitting corrosion resistance under the tested conditions.

Pitting corrosion susceptibility of AL6XN (NO8367) at the Weldment could be attributed to some welding defects; the general body area of the steel has very good pitting corrosion resistance in sea water.

Acknowledgements

The work was performed at the Corrosion Laboratory, McMaster University, Hamilton, Ontario, Canada in collaboration with Prof. M.B. Ives.

References

1. C.A. Loto, and M.B. Ives, Corrosion resistance of super stainless steels in sea water'. Submitted to Corrosion Jnl., June, 1992.
2. A.J. Sedriks, "Corrosion of stainless steels", Wiley Interscience, 1979, pp.70-74.
3. Z. Skzlarzka-Smialowska, "Pitting Corrosion of Metals", NACE, 1986, pp. 145-156.
4. J.R. Ambrose, Corrosion, 34, P.27, (1977).
5. T.P. Hoar, J. Electrochemical Soc. 117, P. 170, (1970).
6. J.E. Truman, M.J. Coleman, K.R. Pirt, Brit. Corr. J. 12, 236, (1977).
7. J. Eckenrod, C.W. Kovack, ASTM STP 679 (Philadelphia, PA, 1977), P. 17.
8. R. Bandy, D. Van Rooyen, Corrosion, 39, 227 (1983).
9. A.J. Sedriks, Mtl. Metall. Reviews 28, 306, (1983).
10. K. Qsozawa, N. Okato, in "Passivity and its Breakdown on Iron and Iron Based Alloys". (NACE, Houston, TX 1976), P. 135.

TABLE 1

CHEMICAL COMPOSITION OF SUPER AUSTENITIC STAINLESS STEELS

Tube No	Alloy/UNS	ELEMENT %										
		Cr	Ni	Mo	Cu	Mn	C	P	S	Si	N	
1	904L(NO8904)	19.0-23	25.0	4.5	1.5	2.0	0.02	0.045	0.035	1.0		
2&5	254SMO (S31254)	19.5-20.5	18.0	6.25	1.0	1.0	0.02	0.03	0.01	0.20		
3&7	AL6XN (NO8367)	20.0-22	24.5	6.5		2.0	0.03	0.04	0.03	1.0	0.23	
4&6	1925HMO (NO8925)	24.0-26	20.0	6.5	1.0	1.0	0.02	0.045	0.03	0.5	0.20	
8	316L(S31603)	16-18	10-14	2-3		2.0	0.03	0.045	0.03	1.0		
9	Dummy	(Any of the above - as specified).										

TABLE 2

TEST CONDITIONS

Run #	Days	Steam Temp.(°C)	Water flow rate (l/s)
4	59	140-160	4.5
5	64	162	4.5
6	61	160	9
7	60	130	1
8	61	160	9

LIST AND LEGENDS FOR THE FIGURES

FIGS.

LEGENDS

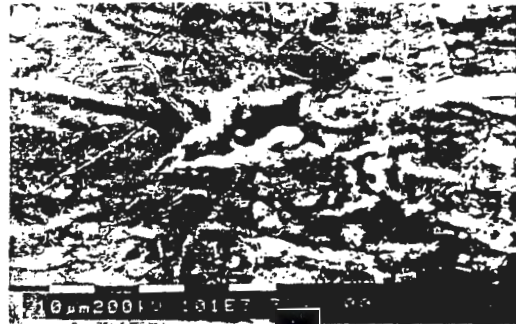
- 1(a) S.E.M. Micrograph of the as-received inner surface of AL6XN (NO8367) alloy tube.
- (b) S.E.M. Micrograph of the corroded inner surface of AL6XN alloy exposed to sea water environment.
- 2(a) S.E.M. Micrograph of the as-received inner surface of 316L (S316603) alloy tube.
- (b) S.E.M. Micrograph of the corroded inner surface of 316L alloy tube.
3. Optical microscope photograph of the split and cleaned tested alloy tubes exposed to sea water in a specially designed test rig.
- 4(a&b) S.E.M. micrographs of two different features of microscopic corrosion pits on the inner surface of AL6XN (NO8367) alloy tube exposed to sea

water environment in the test rig.

5. S.E.M. micrograph of a local corrosion attack site on inner surface of 1925HMO (NO8925) alloy tube exposed to sea water in the test rig.
6. S.E.M. micrograph of the inner surface of the tested 254SMO (S31254) alloy tube showing a ring form of local corrosion attack.
7. S.E.M. micrograph of the microscopic pit on the inner surface of 316L alloy tube used exposed to sea water in the test rig.
8. S.E.M. micrograph of the biofouling/biological materials in the outlet portion of the inner surface of 904L (NO8904) alloy tube, within which bacteria and other microorganisms were located.
9. S.E.M. micrograph of the biological materials in the outlet portion of the inner surface of AL6XN (NO8367) alloy tube within bacteria were located.
10. S.E.M. micrograph of the less dense biological materials at the steam chamber on the inner surface 316L alloy tube showing the presence of bacteria.
11. S.E.M. micrograph of the less dense biological materials at the steam chamber on the inner surface of 316L alloy tube showing the present of bacteria (at higher magnification).
12. EDAX analysis of the biofilm in the outlet portion of 316L (S31603) alloy tube.
13. X-ray diffraction spectroscopy (XRD) analysis of the biofilm obtained from the outlet portion of AL6XN (S08367) alloy tube.



(a)

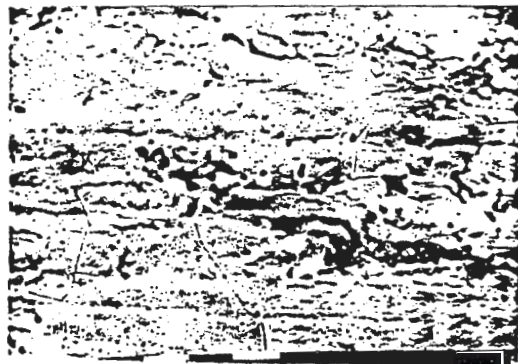


(b)

FIG. 1



(a)



(b)

FIG. 2.

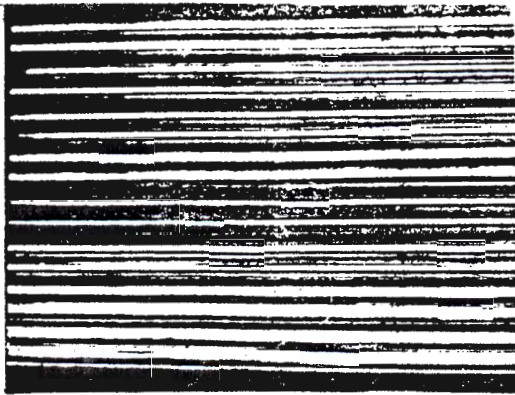


FIG. 3.



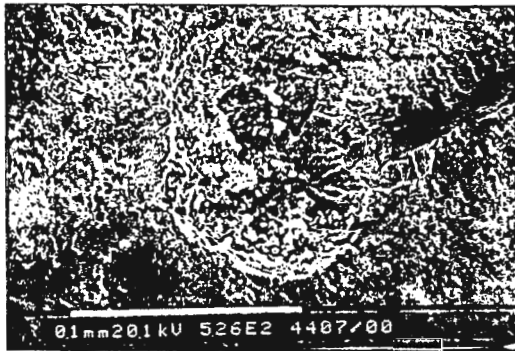
FIG. 6.



(a)



FIG. 7.



(b)

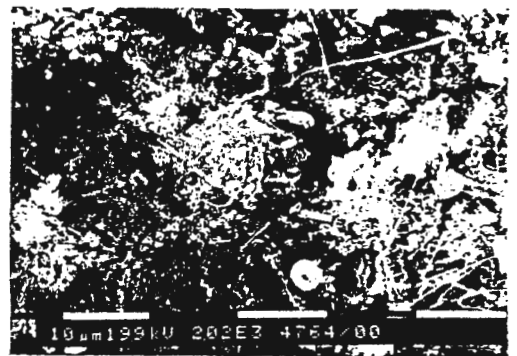


FIG. 8

FIG. 4.

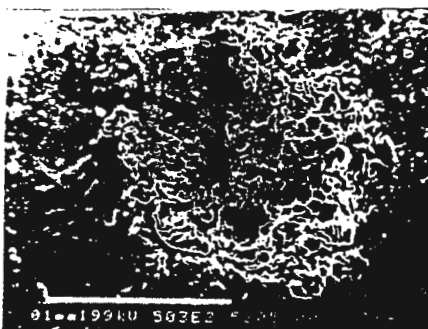


FIG. 5



FIG. 9



FIG. 10.

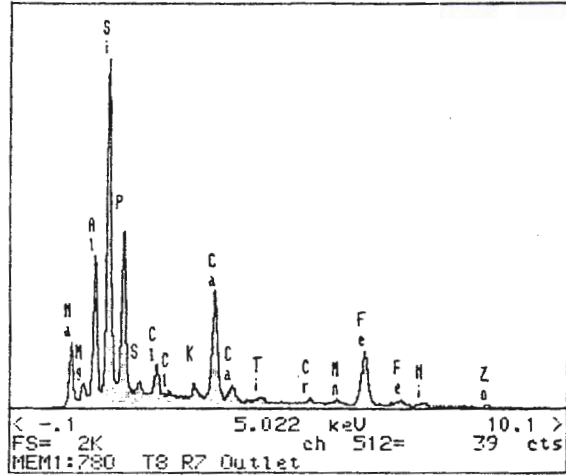


FIG. 12



Fig-11.

